

RESEARCH PAPER

Plant-mediated synthesis of selenium nanoparticles using *Caccinia macranthera* extract and assessment of their antioxidant and cytotoxic properties

Leili Hosseinpour¹, Javad Baharara^{1*}, Saeed Zaker Bostanabad², Majid Darroudi^{3,4}

¹Department of Biology, Mashhad Branch, Islamic Azad University, Mashhad, Iran

²Department of Biology, Parand Branch, Islamic Azad University, Tehran, Iran

³Nuclear Medicine Research Center, Mashhad University of Medical Sciences, Mashhad, Iran

⁴Department of Medical Biotechnology and Nanotechnology, School of Medicine, Mashhad University of Medical Sciences, Mashhad, Iran

ABSTRACT

Objective(s): The current study aims to achieve synthesized selenium nanoparticles (Se-NPs) through a green chemistry route using sodium selenite (Na_2SeO_3) and *Caccinia macranthera* (*C. macranthera*) plant extract as stabilizing and reducing agents and to investigate the anticancer effects of the synthesized NPs.

Materials and Methods: The outcomes affirmed the successful production of the synthesized Se-NPs, as their spherical framework and particle size scale of 54 to 60 nm were exhibited by the images of FESEM/PSA. This spherical frame was also detected in the TEM images at a size of 11.5 nm. The inhibitory effect of Se-NPs was investigated on the proliferation of human liver cancer cells (Huh-7). Additionally, the effect of Se-NPs was studied on the expression of the implicated genes throughout the cell apoptosis using the Real-Time PCR technique. Also, the percentage of apoptotic cells was obtained using Annexin V/PI and DAPI kits. Finally, flow cytometry was exerted to determine the amount of produced ROS.

Results: The results of laboratory studies showed that Se-NPs can significantly reduce the survival of Huh-7 cancer cells in dosage and time-reliant behavior, while they have very little toxicity on normal L929 cells. Also, Se-NPs were able to induce apoptosis in liver cancer cells, which was observed along with the increased expression of Bax, p53, Caspase3, and Caspase 9 genes. In addition, Se-NPs increased the production of ROS in Huh-7 cells and led to an increase in oxidative stress in these cells.

Conclusion: Therefore, these NPs can be used in clinical studies of liver cancer.

Keywords: Antioxidants, Apoptosis, *Caccinia macranthera* plant, Cytotoxins, Selenium nanoparticles

How to cite this article

Hosseinpour L, Baharara J, Zaker Bostanabad S, Darroudi M. Plant-mediated synthesis of selenium nanoparticles using *caccinia macranthera* extract and assessment of their antioxidant and cytotoxic properties. *Nanomed J.* 2024; 11(3): 268-279.

DOI: [10.22038/NMJ.2024.77264.1882](https://doi.org/10.22038/NMJ.2024.77264.1882)

INTRODUCTION

Cancer is a disease which is the cause of mortality of a large number of people every year. Rather than being expensive, traditional treatment methods such as chemotherapy cause serious damage to healthy body cells and have many side effects. Therefore, searching for an effective, low-cost, compatible, and low-risk method is a priority for conducting research [1]. Cancer is caused by the abnormal development

of cells, which is accompanied by changes in cell physiology, these changes include the ability to stimulate angiogenesis, self-sufficiency in growth signals, and no limitation in replication, metastasis, and resistance to apoptosis. Apoptosis is referred to the programmed cell death in which the organism acts to eliminate unwanted cells that threaten the survival of the cell. Any disturbance in the process of apoptosis leads to disease [2].

Recently with the help of nanoparticles, drugs can be transferred to the target organ in a targeted manner and affect certain cells of a tissue. Colloidal stability and cytotoxicity are the two characteristics that can face impacts through the kind of applied

* Corresponding authors: Emails: baharara78@gmail.com; darroudim@mums.ac.ir; majiddarroudi@gmail.com

Note. This manuscript was submitted on January 3, 2024; approved on February 12, 2024

surface coating on nanoparticles. In relation to metal nanoparticles, a natural agent should be used to stabilize the homogeneous state of the solution so that it has both a regenerating state and a powerful coating for metal nanoparticles. The goal of the green technology project is to minimize its potential risks to humans and the environment. Throughout the last decade, the synthesis of Se-NPs as a strong antioxidant has received much attention. Due to its small size, this nanoparticle can easily communicate with cells and tissues at the molecular level. Reducing drug resistance, reducing drug dosage, and creating more efficiency in tumor diagnosis, tumor targeting and treatment, biocompatibility, and biodegradability are some of the parameters behind the suitability of Se-NPs for clinical applications involving cell therapy, tissue restoration, and drug delivery. One of the engrossing and noteworthy topics of nanotechnology is the performance of green synthesis through the collaborated exertion of organic and biodegradable plant-extracted agents, that contain reducing and trapping abilities, with certain metals similar to selenium [1]. Until now, biological production of Se-NPs has been done by plants such as *Rosmarinus officinalis* [3], *Cordia myxa* [4], *Ceropegia bulbosa* [5], *Abelmoschus esculentus* [6], and many other plants.

Although many nanoparticles such as Silver Nanoparticles [7], cobalt oxide nanoparticles [8], and Ag-doped ZnO/MgO nanocomposites [9, 10] have been synthesized using *C. macranthera* plant, no research has been done on the cytotoxicity and antioxidant effect of Se-NPs synthesized by *C. macranthera* plant extract, which indicates the novelty of this research.

The *C. macranthera* plant belongs to the Boraginales order, *Boraginaceae* family, and *Caccinia* genus and *C. macranthera species* [11]. *C. macranthera* plant is an herbaceous perennial plant with a thick and tuberous root whose diameter reaches up to 10 cm. In this research, the root of this plant was used for the synthesis of Se-NPs [7]. By selecting the root of the *C. macranthera* plant as the source material, the aim was to explore a distinct component of the plant, which may have unique bioactive compounds. Plant roots possess specialized functions, such as nutrient absorption, anchoring, and storage. These functions necessitate the presence of various phytochemicals and secondary metabolites that differ from those found in the aerial parts

of the plant. We hypothesized that bioactive compounds present in plant roots, especially in *C. macranthera* extract, may provide benefits in reducing and stabilizing metal nanoparticles, such as Se-NPs. Furthermore, exploiting plant roots could provide a viable alternative for extracting bioactive compounds compared to the more commonly used aerial parts. This approach aligns with sustainable and green chemistry principles, as it minimizes the need for invasive harvesting and excessive use of plant biomass. This research was designed to investigate the cytotoxic effect of Se-NPs synthesized by *C. macranthera* plant extract on the Huh-7 cell line and also investigate the apoptotic and antioxidant effects of these nanoparticles.

Recently, there have been many studies on the anticancer effect of metal nanoparticles synthesized by the green method, however, no research has been done regarding the cytotoxicity and antioxidant effect of Se-NPs synthesized by *C. macranthera* plant extract on Huh-7 and L929 cells, that these show the novelty of the present research.

MATERIALS AND METHODS

Materials

We bought 3-(4,5-Dimethylthiazol-2-yl)-2,5-Diphenyltetrazolium Bromide (MTT), RPMI 1640 (Gibco, USA), Penicillin/streptomycin (Sigma, USA), 0.25% Trypsin-0.05% EDTA solution (Biogene, Iran), Sodium selenite (Na_2SeO_3), Fetal bovine serum (FBS), and DMSO from Merck and Sigma companies. We also provided the newly harvested roots of the *C. macranthera* plant from innate habitation and local markets.

Preparation of extraction

The roots of *C. macranthera* were gathered from the surrounding of its habitat area, Dargaz, Razavi Khorasan, Iran (Banks & Sol.). We washed the roots through the utilization of deionized water and had them dried within the dim. At that point, solvent water (100.0 mL) was used to blend 1.0 g under shaking conditions at 50 °C for the duration of 2 hr. Once the extracted product was sifted through filter paper, we kept the final Residue at 4 °C [4].

Phytochemical analysis

The plant extract was subjected to qualitative phytochemical screening [12].

A) Flavonoids test

To detect the presence or absence of flavonoids, 1 mL of sodium hydroxide (2 N sodium hydroxide) was added to 4 mL of the extract. Sodium hydroxide was prepared by dissolving 4 g in 50 mL of distilled water. The formation of an intense yellow color confirms the presence of flavonoids.

B) Phenolic test

To detect the presence of phenol in the extract, 5 mL of the extract was added dropwise to iron chloride. The formation of a blue-black color revealed the presence of phenolic compound.

C) Tannin test

To perform the tannin test, 4 mL of the extract was transferred to test tubes, to which 3 mL of freshly prepared 10% lead acetate was added dropwise. The formation of a bulky white precipitate confirmed the presence of tannins [13].

Synthesis of selenium nanoparticles

To start the synthesis of Se-NPs, we combined 0.263 g of Na₂SeO₃ with water solvent (100 mL) to go through blending for 15 min. Thereafter, 20 mL of *C. macranthera* extract was included and dropped shrewdly to the salt arrangement up to the point of achieving a clear brown (dark yellow) arrangement, which demonstrated the generation and amalgamation of Se-NPs. The blend of yellow fluid was put under shaking conditions at 60 °C for 60 min to produce an orange colloid arrangement; the resultant was mixed once again at 25 °C for the duration of 48 hr. The observance of color

shifting from colorless towards red affirmed the production of Se-NPs. At this point, we put our NPs within a freeze dryer at -80 °C for a period of 48 hr [4]. The green synthesis plan of Se-NPs was included in Fig. 1.

Characterization of nanoparticles

Since characterization techniques are the foremost vital parameter regarding the recognition and management of nanoparticle synthesizing procedure and utilization, there is an assortment of analytical strategies for this matter counting XRD, FTIR, UV-Vis, FESEM, EDX, TEM, and DLS/Zeta potential. This technique can facilitate the selective detection of the size and framework of Se-NPs at a stable state. Therefore, the obtained absorption of this case was assessed through the data of UV-Vis spectrophotometers (Beijing Purkinje General Instrument Co.), while the XRD method was simultaneously executed to assay the microcrystals of our product. (Philips Co., Holland). After evaluation of the morphology and size of these materials with FESEM, (Hitachi Co, Japan S4800) EDX analysis was performed with the Oxford IE-150 device to determine the content of the sample. Moreover, the size and stability of NPs were investigated through the DLS/Zeta potential and also were acquired in the Fourier transform infrared (FTIR, Shimadzu 8400, Japan) spectra of *Coccinia macranthera* extract and Se-NPs to recognize the bounded functional groups, specifically on the biosynthesized Se-NPs [3].

Cell culture

We procured a human hepatoma cell line

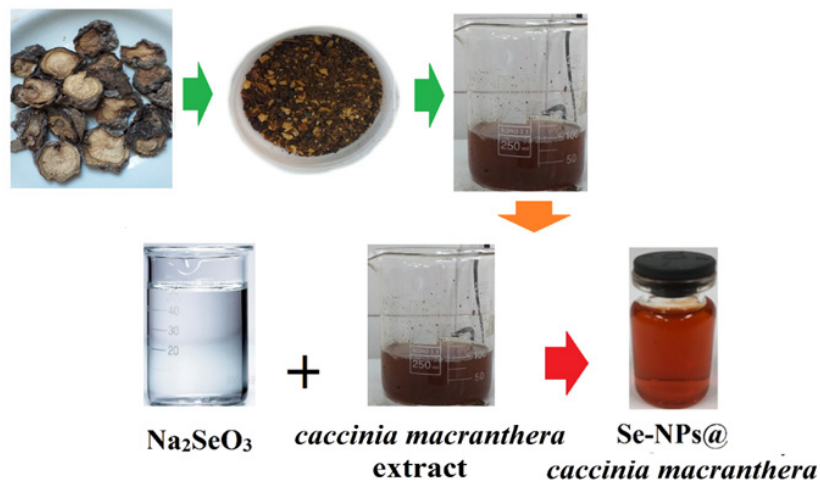


Fig. 1. Schematic plan of plant-based synthesis of Se-NPs

(Huh-7) and a normal cell line (L929) from the Pasteur Institute of Tehran, Iran. By using a complete culture medium, including RPMI 1640 culture medium composed of 10% FBS and 1% penicillin-streptomycin antibiotic, the culturing step was done within special cell culture flasks and incubated at a CO₂ atmosphere (5 %) that contained a corresponding humidity of 95 % at 37 °C [4].

MTT assay

The cytotoxicity of our produced Se-NPs was studied on the Huh-7 and L929 cell lines through the data of MTT assay. First, the seeding of about 1×10^4 cells/within 96-well plates was completed to execute an incubation process in RPMI, 10 % FBS. After 24 hr of incubation for adherence to the plate, the samples were individually introduced to varying volumes of Se-NPs (15.5 to 500 µg/mL). After 24 hr, 5 mg/mL of MTT solution was taken and appended to every well to incubate the plate for 4 hr at the degrees of 37 °C. Thereafter, DMSO (100 µL) was put into each well to perform incubation for 15 min at ambient temperature. Finally, we recorded the absorption rate with an ELISA reader at a wavelength of 570 nm. Every experiment was done five times (n = 5) to gather stronger outcomes with ensured accuracy. In the last stage, the viability and amount of IC₅₀ assessment was evaluated by exploiting the SPSS® and Prism® software [14].

DAPI nuclear staining

In the form of a fluorescent dye, DAPI is capable of firmly binding to adenine-thymine-rich areas in DNA and therefore paves the way for checking the morphology of nuclei by a fluorescent microscope. At first, the culturing of 35×10^4 Huh-7 cells was completed in each well of a 6-well plate to face the mentioned concentrations of Se-NPs (20, 60, and 100 µg/mL) for 24 hr. After that, 1 mL of DAPI solution was separately put into the wells and positioned in an incubator for 15 min. Then, DAPI was removed and 1 mL of methanol was appended to every well to settle the cells [15]. All work steps were performed in the absence of light and the morphology of the cell nucleus was examined by fluorescent microscope (Biomed, Korea).

Measuring the production of oxygen-free radicals

DCFDA/H2DCFDA kit (Abcam) was used to investigate the effect of selenium nanoparticles on the induction of cellular oxidative stress and

ROS production in Huh-7 cancer cells. For this purpose, the culturing of 20,000 Huh-7 cells was done in each well of a 96-well plate, which faced the Se-NPs volumes of 20, 60, and 100 µg/mL after 24 hr. 24 h after the treatment, staining was done by DCFDA with a concentration of 25 µM for 30 min at 37 °C in dark [16]. Finally, the fluorescence data were obtained by PERKIN ELMER fluorimeter through the emission and absorption wavelengths of 485 of 535 nm, respectively.

Annexin V-propidium iodide test for apoptosis

One of the biomarkers of the apoptosis process is the penetration of phosphatidylserine from the interior layer of the plasma membrane toward its exterior layer. Upon the positioning of phosphatidylserine on a cell surface, it can be detected using a fluorescent dye that binds to Annexin V. An Annexin V propidium iodide kit (Abcam) was used to perform this test. First the culturing of 35×10^4 Huh-7 cells was done in each well of a 6-well plate, which then faced the mentioned concentrations of Se-NPs (20, 60, and 100 µg/mL) for a duration of 24 hr. After this period, they were trypsinized and centrifuged at 400 g for 5 min, and thus appended 200 µL of Annexin-Binding buffer (1x) to the cell sediment to perform centrifugation. In the next step, 50 µL of Annexin V-FITC/PI solution was added to the cell sediment to go through incubation for 10 min at ambient temperature in the dark. Then, 150 µL of Annexin-Binding buffer (1x) was added to the resulting suspension, and the reading was done by flow cytometry (BD, USA) [17].

Gene expression analysis

Real-time PCR was exerted to configure the expression levels of Bax, p53, Caspase 3, and Caspase 9 genes. After extracting RNA through an RNA extraction kit (pars tous, Iran), the concentration of RNA to make complementary DNA molecules was determined by the nanodrop device at 260 and 280 nm wavelength, and then cDNA synthesis was performed according to the protocol of the cDNA kit (Pars tous, Iran). Finally, a real-time time-PCR test was done with a Cybergreen kit (SYBR Green Master Mix, pars tous, Iran) [17]. In this study, primers used for Bax, p53, Caspase3, and Caspase9 genes were considered as target genes and the GAPDH gene as internal control (Table 1).

Tab. 1. Primers Sequence

Gene symbol	Gene name	Primers (5' → 3')
Bax	Bcl-2-associated X protein	Forward: CAAAGTGGTCTCAAGGCC Reverse: GAAGCCAATGCCAGCCCA
P53	Tumor suppressor protein	Forward: AACAGCTTTGAGGTGCGTGT Reverse: GTTGGCAGTGCCTCGCTT
Caspase3	Cysteine-aspartic acid protease 3	Forward: TGGAATTGATGCGTGATTTTCT Reverse: ACTTCTACAACGATCCCTCTG
Caspase9	Cysteine-aspartic acid protease 9	Forward: TCCTACTACTTCCAGGTTT Reverse: AAAGCAACGAGCATCTGTT
GAPDH	Glyceraldehyde-3-phosphate dehydrogenase	Forward: TGGAAGGACTCATGACCACAGT Reverse: TTCCCGTTCAGCTCAGGGAT

RESULT AND DISCUSSION

XRD

XRD pattern was used for the determination of crystal structure, purity, and crystallite size of the Se-NPs (Fig. 2). By comparing the XRD pattern of the synthesized Se-NPs with the standard JCPDS (card No # 06-362) [5, 18], it was found that the synthesized Se-NPs are entirely pure and amorphous. Also, due to the absence of narrow peaks with high intensity, the XRD pattern of Se-NPs confirmed their amorphous nature. The gathered results were parallel to the report of Alagesan et al., [18].

UV-Vis/Band gap

A UV-Vis spectrum was captured throughout the scale of 200 to 800 nm to affirm the creation of Se-NPs. The acquired UV-Vis range shows

the accomplishment of NPs blends after 48 h. In coordination to Fig. 3(a), the inclusion of an aqueous extract resulted in the fabrication of red Se-NPs, which were initially incubated for a designated time interval. The UV-Vis range of Se-

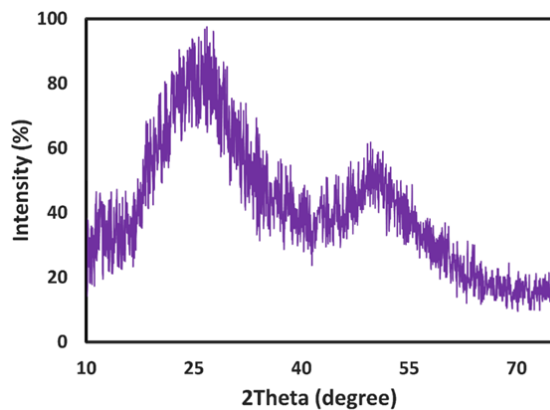


Fig. 2. The XRD pattern of Se-NPs

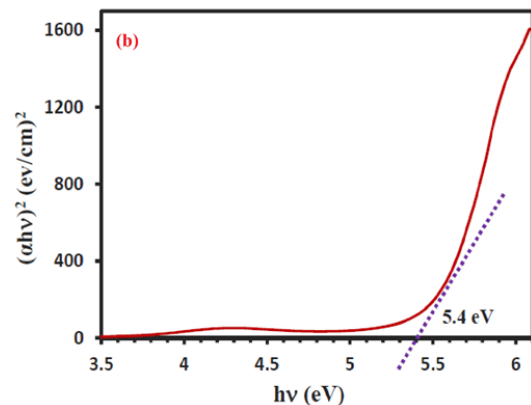
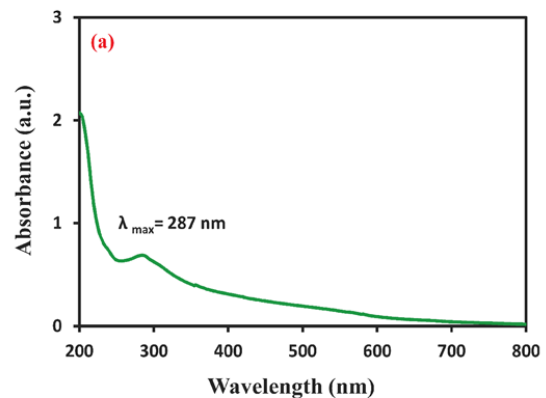


Fig. 3. UV-Vis (a) and Band gap of Se-NPs (b)

NPs was uncovered at 287 nm through the gathered data from the surface plasmon reverberation (SPR) of synthesized Se-NPs. In similarity to recent research, the near situating of conduction and valence groups encourages the flowing of electrons in a free manner, possibly resulting in an increment within the SPR assimilation band [5, 19, 20]. Agreeing with the UV-Vis results information, we configured the bandgap energy (E_g) of our -NPs utilizing Eq. 1, as well as the E_g esteem that was almost 5.4 eV. The graph of $(\alpha h\nu)^n$ in vers is displayed in Fig. 3(b). The gathered outcomes were parallel to the discoveries of Velayati *et al.*, [20-22].

$$(\alpha h\nu) = A(h\nu - E_g)^n \quad (1)$$

In which the ν and α are the light frequency and light absorption coefficient, respectively. A , and n are constant, and the value of n and band gap values are specified by the transition type of the Se-NPs.

DLS/ Zeta potential test

Dynamic light scattering (DLS) is used to compute the size of dispersed Se-NPs throughout the solution. (Fig. 4 (a, b)). Agreeing with the DLS test, the NPs have a size of about 162-193 nm and a PDI equal to 0.345. Zeta potential alludes to the point of genuine electric charge at the surrounding of nanoparticles surface. The zeta potential value of the synthesized Se-NPs was obtained to be 21.3 mV, which approved the high stability of our product. Our discoveries were approved to follow Adibian *et al.*, and Ghaderi *et al.* outcomes [23, 24].

TEM Image

We inspected the framework and measure of

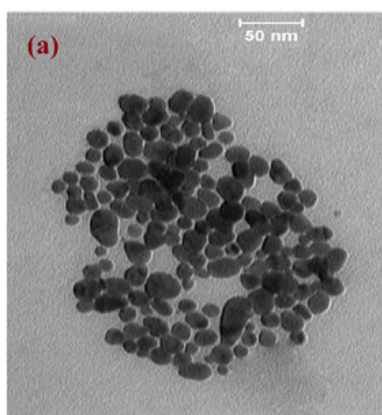


Fig. 5. TEM (a) and Particle size distribution curve according to TEM image (b)

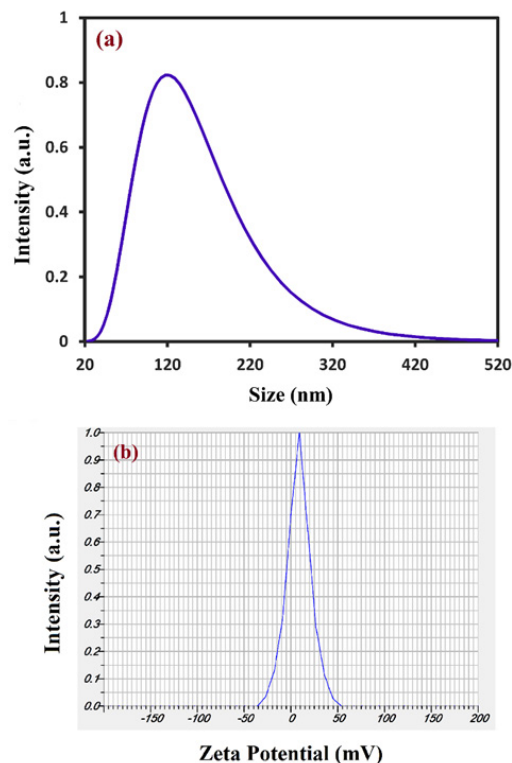
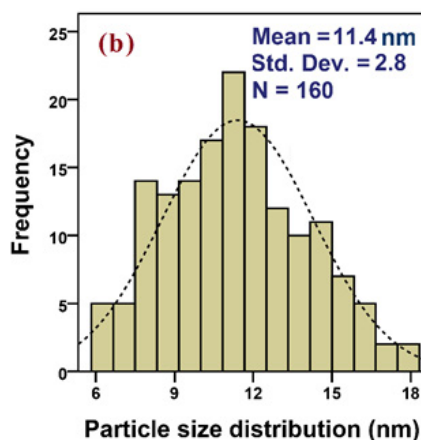


Fig. 4. DLS (a) and Zeta potential (b) of NPs

these nanoparticles through the exertion of TEM/ PSA examinations. The TEM pictures showed the achievement of a round framework (Fig. 5a) that was finely scattered all through the extraction of *C. macranthera*, while the PSA histogram (Fig. 5b) was demonstrative of a normal estimate of around 11.5 nm.

FESEM/EDX/PSA

The FESEM image of nanoparticles are show in



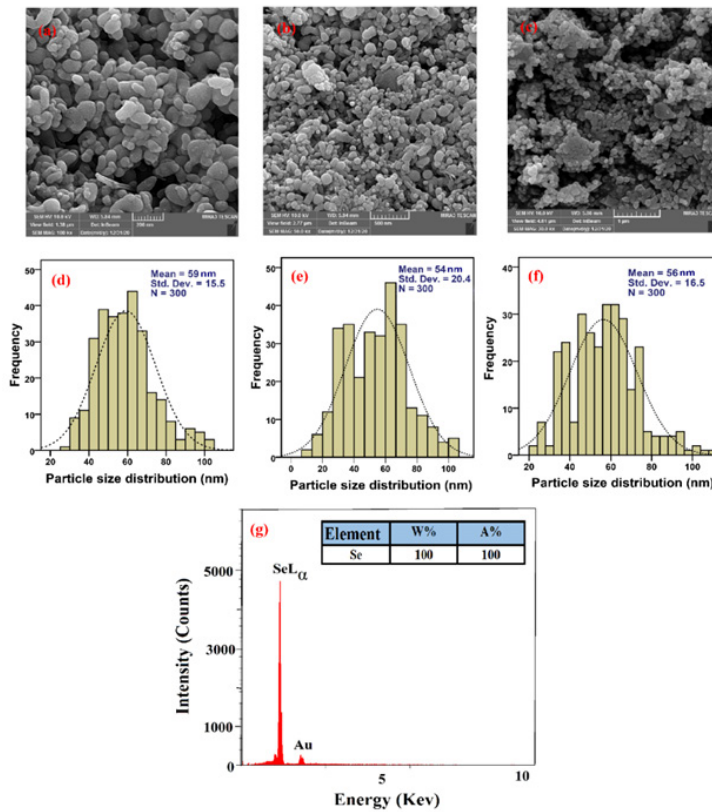


Fig. 6. FESEM images (a-c), Particle size distribution curve according to FESEM images (d-f), and EDX analysis of Se-NPs (g)

Fig. 6(a-c). They confirmed the formation of stable and circular shapes of our product. The EDX test confirmed the existence of the Se element (Fig. 6(g)). The EDX test showed the Se peak, which confirmed the existence of the Se element. The size of our product was configured through PSA investigation and was almost 54-60 nm (Fig. 6(d-f)). As it is known, capping and stabilizing agents are responsible for preventing the uncontrollable growth of NPs and inhibiting particle aggregation. Ghaderi *et al.* detailed the recognition of a circular frame throughout a similar case of Se-NPs synthesis as comparable data with our outcomes [24].

FTIR

To assign the presence of stabilizer in Se-NPs synthesized in the substrate of *C. macranthera* plant extract, FTIR coverage was investigated in the range of 400-4000 cm^{-1} , and their results are presented in Fig. 7. According to the FTIR spectrum of *C. macranthera* extract, a strong peak is observed in the 3430 cm^{-1} region, which is connected to the stretching vibration of OH group and the peak at 2920 cm^{-1} is related to the stretching vibration of the CH group. The

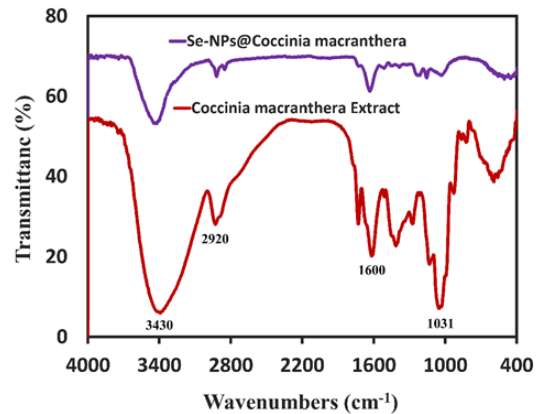


Fig. 7. FTIR spectrum of extracted *C. macranthera* and Se-NPs

absorption band in the 1031 cm^{-1} is associated with the C-O-C group. According to the FTIR spectrum of Se-NPs, we can see that the absorption band of the OH group has shifted from 3430 cm^{-1} in the extract to 3420 cm^{-1} and the intensity of the peak is shorter, which shows that free hydroxyl groups in *C. macranthera* extract are involved with Se-NPs. Also, the peak intensity related to CH vibrations of Se-NPs (2920 cm^{-1}) is slightly reduced compared to the spectrum of *C. macranthera* extract (2930 cm^{-1}).

The observed band in 1600 cm^{-1} is related to the stretching vibrations of the COO- and C-O-C groups and the peak intensity of Se-NPs has also been decreased compared to the extract. Thus, the FTIR spectrum of Se-NPs is similar to the spectrum of *C. macranthera* extract. These facts confirm the connection of *C. macranthera* extract compounds with Se-NPs and show that the stabilizing agent is a part of Se-NPs and that *C. macranthera* can well protect against the accumulation of Se-NPs [14].

In vitro study of Se-NPs

In this test, the survival percentage of Huh-7 cells treated with Se-NPs was investigated. The results indicate the concentration and time-dependent inhibitory function of Se-NPs on the growth of liver cancer cells. The obtained results show that the IC_{50} value after 24 hr was about $85\text{ }\mu\text{g/mL}$, at 48 hr about $43\text{ }\mu\text{g/mL}$, and after 72 hr about $31\text{ }\mu\text{g/mL}$. According to the calculations, it was concluded that the level of toxicity is a function of concentration, which decreases with decreasing concentration. The results of investigating the cytotoxicity of Se-NPs synthesized by *C. macranthera* plant extract on the normal cell line L929 showed that this nanoparticle in high concentrations (500 and $250\text{ }\mu\text{g/mL}$) and long-term treatment (72 hr) can have a moderate toxic effect on normal cells, while in lower concentrations, its toxicity is very low (Fig. 8). Several similar studies have studied the toxicity effects of Se-NPs on different cancer cell lines [25, 26]. However, the impacts of our product cytotoxicity on the Huh-7 liver cancer cell line have not been studied so far.

Past research also showed that among many types of nanoparticles, Se-NPs have selective anticancer activity on cancer cells and have little toxicity to normal cells [27]. In the discussion of drug delivery and cancer treatment, most anti-cancer drugs cannot discern the difference between normal and cancerous cells, and consequently, their prescription is required to be in high doses to reach the targeted site of the tumor, and this high dose of the drug in the tumor area leads to severe side effects. Nanostructures with a hydrophilic surface at sizes below 100 nm proved to contain the strongest escaping property from the molecular phagocytic system. Endoplasmic reticulum organs are capable of devouring hydrophobic nanoparticles at a high speed. Based on the findings of this research,

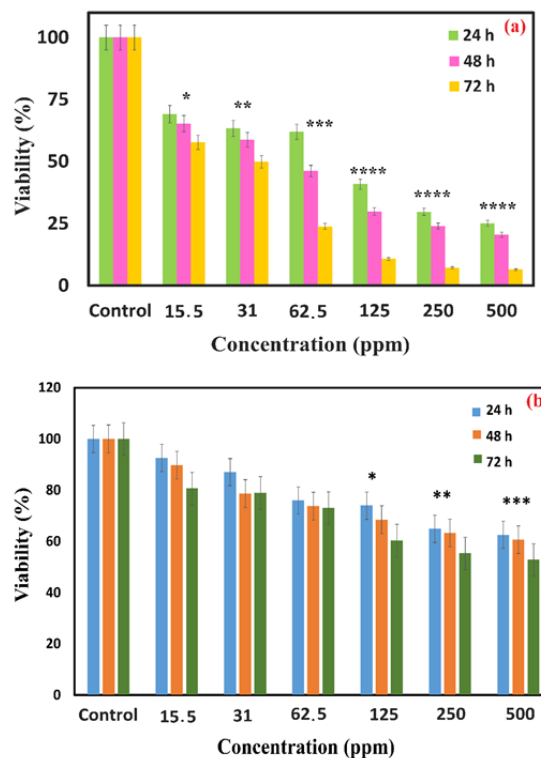


Fig. 8. The viability of Se-NPs towards Huh-7 (a) and L929 (b) cells, (* $P<0.05$, ** $P<0.01$, *** $P<0.001$, and **** $P<0.0001$)

the Se-NPs synthesized in the water bed of the *C. macranthera* plant are hydrophilic and their size is about 11.5 nm, therefore, they can stay longer in the blood circulation. In coordination with recent assessments, the low dosages of nanomaterials proved to be quite biocompatible, whereas the higher dosages of nanomaterials can stand as a severe threat to normal or healthy cells [28].

DAPI staining results

The results of DAPI staining showed that the treatment by the varying volumes of our product, which was synthesized with *C. macranthera* extract ($20, 60, \text{ and } 100\text{ }\mu\text{g/mL}$), caused fragmentation of the nucleus of the cells, which indicates the induction of apoptosis in the cells. As shown in Fig. 9, these cellular changes were increased due to the increase in the concentration of Se-NPs, and at the concentration of $100\text{ }\mu\text{g/mL}$, the most fluorescent color is evident and these results are similar to previous research [29, 30].

Selenium nanoparticles, induced apoptosis in Huh-7 cells

At this stage, apoptosis was investigated using

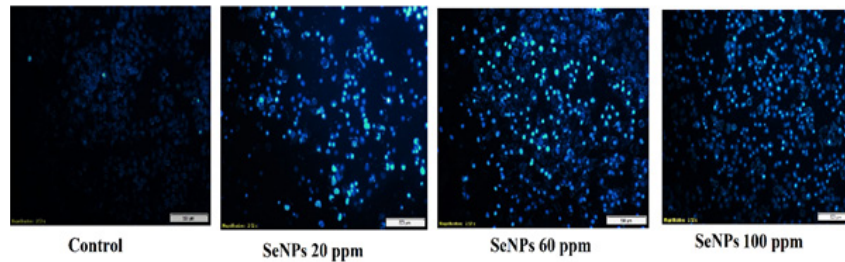


Fig. 9. Qualitative effect of apoptosis induction by Se-NPs by DAPI staining method in Huh-7 cells

Annexin-V and PI double staining kit in the Huh-7 cell line (Fig. 10). One of the key mechanisms of nanoparticles, including Se-NPs that can induce the toxicity and death of cancerous cells, is the ability of these particles to produce reactive oxygen species and induce oxidative stress due to the accumulation of NPs in cancer cells. Several evidences indicate that cancer cells produce more ROS than normal cells and are exposed to oxidative stress. In previous studies *in vitro* and *in vivo* models, it has been observed that Se-NPs have the ability to destroy cancer cells and prevent tumor growth due to a significant increase in the fabrication of ROS [30]. The present study implicated the effect of Se-NPs synthesized using the *C. macranthera* plant on the amount of ROS

production in Huh-7 cancer cells. The results of flow cytometers indicated that the amount of ROS production increased significantly succeeding to 24 h of treating Huh-7 cells by Se-NPs throughout a concentration-reliant attitude (Fig. 10a). Our gathered data show that the occurrence of apoptosis in liver cancer cells under the influence of Se-NPs is probably due to the increase in ROS production and oxidative damage in these cells, and will eventually cause the initiation of apoptotic pathways caused by oxidative stress.

In addition to stimulating apoptosis, nanoparticles can stimulate other modes of cell death such as autophagy and necrosis in cancer cells. However, as with other anticancer drugs, the main mechanism of anticancer activity of

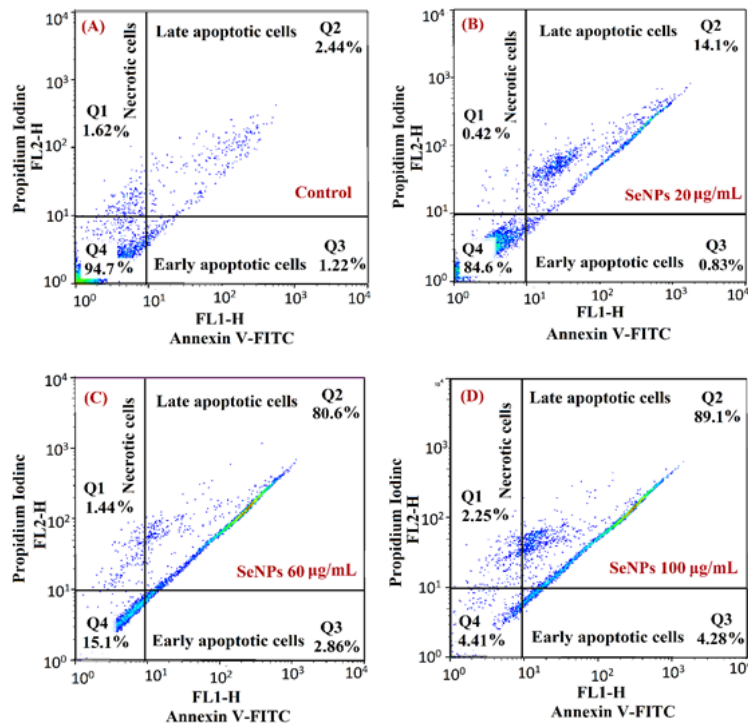


Fig. 10. Apoptotic functional of Se-NPs on Huh-7 cell line. A: Flow cytometric result of Huh-7 cancer cell as the control without the presence of Se-NPs. B-D: Flow cytometric results of the effect of Se-NPs synthesized with *C. macranthera* extract (20, 60, and 100 µg/mL) after 24 hr. (Q1 : necrotic cells, Q2: Late apoptotic, Q3: early apoptotic, Q4: viable cells)

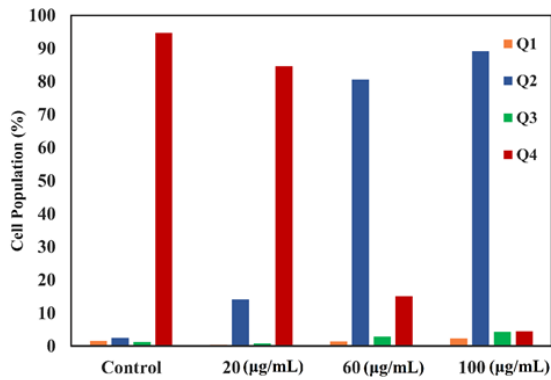


Fig. 11. Comparison of the percentage of necrotic cells, early and late apoptotic cells in the flow cytometry results, obtained from the treatment of Se-NP nanoparticles synthesized with *C. macranthera* extract (20, 60 and 100 µg/ml), after 24 hr (Q1: necrotic cells, Q2: Late apoptotic, Q3: early apoptotic, Q4: viable cells)

the nanoparticles is the induction of apoptosis in cancer cells. In coordination with the outcomes of our research, increasing the concentration of Se-NPs synthesized by *C. macranthera* plant extract in the Huh-7 cell line relatively increased the secondary apoptosis rate which indicates the transfer of phosphatidylserine from the interior surface towards the exterior part of plasma membrane due to cell destruction. Further research on the molecular mechanisms also shows the stimulation of apoptosis by the activation of Caspase3 in this study. The graph of the flow cytometry results including the percentage of necrotic cells, early, and late apoptotic cells are shown in Fig. 11.

Gene expression analysis

According to the results of Real-Time PCR, it was found that Se-NPs significantly change the expression of apoptotic genes. In this way, the treatment of Huh-7 cells with Se-NPs seems to intensify the expression of Bax, p53, Caspase3, and Caspase9 genes compared to the GAPDH reference gene, which is consistent with the findings of other past studies [31]. Previous studies showed that the p53 factor plays an essential role in the cellular response to DNA damage and apoptosis caused by increased ROS and oxidative stress. In general, the p53 protein is inactive and in low concentrations in cells, and when the cells are stressed, the increase in the level of this factor leads to the blocking of the cell cycle progress. This phenomenon can provide time for DNA repair or the cell moves towards apoptosis. In addition,

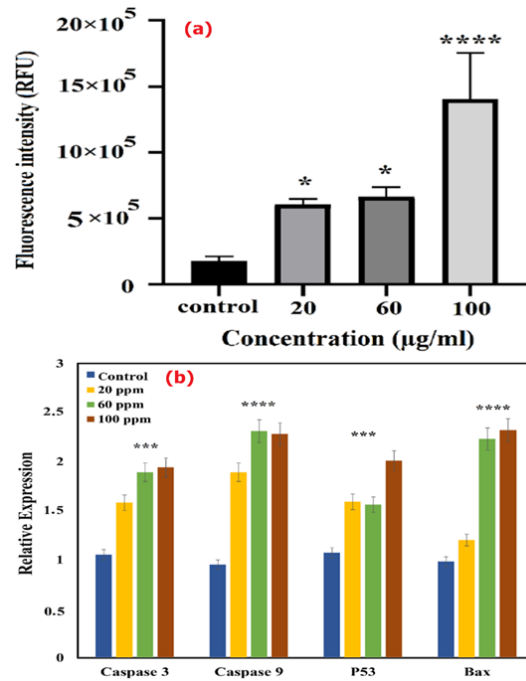


Fig. 12. Effect of Se-NPs on the production of oxygen free radicals on Huh-7 cells after 24 h incubation (a) and Effect of Se-NPs on the expression of Bax, p53, Caspase3, and Caspase9 genes in Huh-7 cells (b). (* $P < 0.05$, ** $P < 0.01$, *** $P < 0.001$, and **** $P < 0.0001$)

the p53 protein can induce the mitochondrial pathway of apoptosis by inhibiting the expression of anti-apoptotic protein Bcl-2 and intensifying the expression of pro-apoptotic protein Bax. It is also assumed that the activation of the p53 protein, followed by the increase in Bax levels, has a direct role in accelerating the release of apoptosis-inducing factors from mitochondria, such as cytochrome C, and finally, the activation of the Caspase cascade. According to the above reports, in the present study, the influence of Se-NPs on the expression of apoptotic genes Bax, p53, Caspase 3, and Caspase 9 in Huh7 cells was observed (Fig. 12b) [31, 32]. The results indicated an increase in the expression of the mentioned genes by Se-NPs synthesized from *C. macranthera* plant extract, which is consistent with the findings of other past studies [29, 32].

CONCLUSIONS AND FUTURE WORK

According to recent research, Se-NPs can enter the cells through receptor-mediated endocytosis due to their small size. Cancer cells have acidic pH with redox imbalance. Se-NPs cause the formation of more free radicals, which may unsettle the

mitochondrial membrane and lead to the leakage of mitochondrial proteins, as well as induce endoplasmic reticulum stress. Mitochondrial membrane unsettlement and protein leakage cause the activation of Caspases and ultimately, destructive cellular events will cause DNA fragmentation, stop the cell cycle, and finally cell death. In this study, according to the findings of flow cytometry, the anticancer activity of Se-NPs against Huh-7 cells and the increased expression of pro-apoptotic genes, it can be claimed that Se-NPs can cause the death and removal of cancer cells, while these nanoparticles can be antioxidants in the face of natural cells and have a protective role. The superb antioxidant power of plant-sourced Se-NPs is attributable to the superior level of nano selenium, which is quite essential for increasing selenoenzymes such as glutathione peroxidase and thioredoxin reductase, which help protect cells and tissues inside the body against free radicals. Therefore, Se-NPs synthesized in this treatise can be used as a promising strategy in studies related to the field of cancer and liver cancerous therapy. Our recommendation for further work is to investigate the possible effects of Se-NPs on other factors related to carcinogenesis mechanisms, such as genes and proteins involved in the pathways of metastasis or angiogenesis of cancer cells.

ACKNOWLEDGMENTS

The technical support for this work was provided by the Islamic Azad University of Mashhad and the University of Medical Sciences of Mashhad based on the Ph.D. thesis of Mrs. Leili Hosseinpour.

CONFLICTS OF INTERESTS

The authors declare no competing interests.

REFERENCES

1. Garcia-O P, Otero P, Pereira AG, Chamorro F, Carpena M, Echave J, et al. Status and challenges of plant-anticancer compounds in cancer treatment. *Pharmaceuticals*. 2021; 14(2):157-169.
2. Carneiro BA, El-Deiry WS. Targeting apoptosis in cancer therapy. *Nat Rev Clin Oncol*. 2020; 17(7):395-417.
3. Adibian F, Ghaderi RS, Sabouri Z, Davoodi J, Kazemi M, Ghazvini K, et al. Green synthesis of selenium nanoparticles using *Rosmarinus officinalis* and investigated their antimicrobial activity. *BioMetals*. 2022; 35(1):147-158.
4. Hosseinpour L, Baharara J, Bostanabad SZ, Darroudi M. Plant-based synthesis of selenium nanoparticles using *Cordia myxa* fruit extract and evaluation of their cytotoxicity effects. *Inorg Chem Commun*. 2022; 145:110030.
5. Cittrarasu V, Kaliannan D, Dharmar K, Maluventhen V, Easwaran M, Liu WC, et al. Green synthesis of selenium nanoparticles mediated from *Ceropegia bulbosa* Roxb extract and its cytotoxicity, antimicrobial, mosquitocidal, and photocatalytic activities. *Sci Rep*. 2021; 11(1):1-15.
6. Ghaderi RS, Adibian F, Sabouri Z, Davoodi J, Kazemi M, Amel Jamehdar S, et al. Green synthesis of selenium nanoparticle by *Abelmoschus esculentus* extract and assessment of its antibacterial activity. *Mater Technol*. 2022; 37(10):1289-1297.
7. Khojasteh-Taheri R, Ghasemi A, Meshkat Z, Sabouri Z, Mohtashami M, Darroudi M. Green synthesis of silver nanoparticles using *Salvadora persica* and *Caccinia macranthera* extracts: Cytotoxicity analysis and antimicrobial activity against antibiotic-resistant bacteria. *Appl Biotechnol Biochem*. 2023; 195(8):5120-5135.
8. Mohandes A, Aghamaali MR, Sabouri Z, Darroudi M. Biosynthesis of cobalt oxide nanoparticles (Co₃O₄-NPs) using *Caccinia macranthera* extract and evaluation of their cytotoxicity and photocatalytic activity. *Mater Sci Eng*. 2023; 297:116782.
9. Sabouri Z, Sabouri S, Tabrizi Hafez Moghaddas SS, Mostafapour A, Amiri MS, Darroudi M. Facile green synthesis of Ag-doped ZnO/CaO nanocomposites with *Caccinia macranthera* seed extract and assessment of their cytotoxicity, antibacterial, and photocatalytic activity. *Bioprocess Biosyst Eng*. 2022; 45(11):1799-1809.
10. Sabouri Z, Sabouri S, Moghaddas S, Mostafapour A, Gheibihayat SM, Darroudi M. Plant-based synthesis of Ag-doped ZnO/MgO nanocomposites using *Caccinia macranthera* extract and evaluation of their photocatalytic activity, cytotoxicity, and potential application as a novel sensor for detection of Pb²⁺ ions. *Biomass Convers Biorefin*. 2022; 14(1):1-13.
11. Akbar S, *Caccinia macranthera* var. *glauca* (Savi) Govaerts (Boraginaceae). *Handbook of 200 Medicinal Plants*. 2020;479-482.
12. Khandel P, Shahi SK, Soni DK, Yadav RK, Kanwar L. *Alpinia calcarata*: a potential source for the fabrication of bioactive silver nanoparticles. *Nano Conver*. 2018; 5:1-17.
13. Shaikh JR, Patil M. Qualitative tests for preliminary phytochemical screening: An overview. *Int J Chem Stud*. 2020; 8(2):603-608.
14. Sabouri Z, Akbari A, Hosseini HA, Khatami M, Darroudi M. Green-based bio-synthesis of nickel oxide nanoparticles in Arabic gum and examination of their cytotoxicity, photocatalytic and antibacterial effects. *Green Chem Lett Rev*. 2021; 14(2):404-414.
15. Pasha A, Kumbhakar DV, Sana SS, Ravinder D, Lakshmi BV, Kalangi SK, et al. Role of biosynthesized Ag-NPs using *Aspergillus niger* (MK503444. 1) in antimicrobial, anti-cancer, and anti-angiogenic activities. *Front Pharmacol*. 2022; 12:4081.
16. Afshari AR, Jalili-Nik M, Soukhtanloo M, Ghorbani A, Sadeghnia HR, Mollazadeh H, et al. Auraptene-induced cytotoxicity mechanisms in human malignant glioblastoma (U87) cells: role of reactive oxygen species (ROS). *EXCLI J*. 2019; 18:576.
17. Amiri H, Hashemy SI, Sabouri Z, Javid H, Darroudi M. Green synthesized selenium nanoparticles for ovarian cancer cell apoptosis. *Res Chem Int*. 2021;47(6):2539-2556.
18. Alagesan V, Venugopal S. Green synthesis of selenium nanoparticle using leaves extract of *withania somnifera* and its biological applications and photocatalytic activities. *Bionanoscience*. 2019; 9(1):105-116.
19. Sabouri Z, Rangrazi A, Amiri MS, Khatami M, Darroudi

- M. Green synthesis of nickel oxide nanoparticles using *Salvia hispanica* L.(chia) seeds extract and studies of their photocatalytic activity and cytotoxicity effects. *Bioprocess Biosyst Eng.* 2021; 44(11):2407-2415.
20. Velayati M, Hassani H, Sabouri Z, Mostafapour A, Darroudi M. Biosynthesis of Se-Nanorods using Gum Arabic (GA) and investigation of their photocatalytic and cytotoxicity effects. *Inorg Chem Commun.* 2021; 128:108589.
21. Velayati M, Hassani H, Darroudi M. Green synthesis of Se-Nanorods using Poly Anionic Cellulose (PAC) and examination of their photocatalytic and cytotoxicity effects. *Inorg Chem Commun.* 2021; 133:108935.
22. Velayati M, Hassani H, Sabouri Z, Mostafapour A, Darroudi M. Green-based biosynthesis of Se nanorods in chitosan and assessment of their photocatalytic and cytotoxicity effects. *Environ Technol Innov.* 2022; 27(8):102610.
23. Adibian F, Ghaderi RS, Sabouri Z, Davoodi J, Kazemi M, Ghazvini K, et al. Green synthesis of selenium nanoparticles using *Rosmarinus officinalis* and investigated their antimicrobial activity. *BioMetals.* 2022; 35(1):147-158.
24. Ghaderi RS, Adibian F, Sabouri Z, Davoodi J, Kazemi M, Amel Jamehdar S, et al. Green synthesis of selenium nanoparticle by *Abelmoschus esculentus* extract and assessment of its antibacterial activity. *Mater Tech.* 2021; 37(10):1-9.
25. Hasanin M, Hassan SA, Hashem AH: Green biosynthesis of zinc and selenium oxide nanoparticles using callus extract of *Ziziphus spina-christi*: characterization, antimicrobial, and antioxidant activity. *Biomass Convers Biorefin* 2021; 13(2):1-14.
26. Varlamova EG, Goltyaev MV, Mal'tseva VN, Turovsky EA, Sarimov RM, Simakin AV et al. Mechanisms of the cytotoxic effect of selenium nanoparticles in different human cancer cell lines. *nt J Mol Med Sci.* 2021; 22(15):7798.
27. Ullah A, Mu J, Wang F, Chan MWH, Yin X, Liao Y, et al. Biogenic Selenium Nanoparticles and Their Anticancer Effects Pertaining to Probiotic Bacteria—A Review. *Antioxidants.* 2022; 11(10):1916.
28. Lin W, Zhang J, Xu J-F, Pi J. The advancing of selenium nanoparticles against infectious diseases. *Front Pharmacol.* 2021; (12):1971.
29. Baharara J, Ramezani T, Divsalar A, Mousavi M, Seyedarabi A. Induction of apoptosis by green synthesized gold nanoparticles through activation of caspase-3 and 9 in human cervical cancer cells. *Avicenna J Med Biotechnol.* 2016; 8(2):75.
30. Wu T, Duan X, Hu C, Wu C, Chen X, Huang J, et al. Synthesis and characterization of gold nanoparticles from *Abies spectabilis* extract and its anticancer activity on bladder cancer T24 cells. *Artif Cells Nanomed Biotechnol.* 2019; 47(1):512-523.
31. Almarzoug MH, Ali D, Alarifi S, Alkahtani S, Alhadheq AM. Platinum nanoparticles induced genotoxicity and apoptotic activity in human normal and cancer hepatic cells via oxidative stress-mediated Bax/Bcl-2 and caspase-3 expression. *Environ Toxicol.* 2020; 35(9):930-941.
32. Katifelis H, Lyberopoulou A, Mukha I, Vityuk N, Grodzyuk G, Theodoropoulos GE, et al. Ag/Au bimetallic nanoparticles induce apoptosis in human cancer cell lines via P53, CASPASE-3, and BAX/BCL-2 pathways. *Artif Cells Nanomed Biotechnol.* 2018; 46(sup3):389-398.